Ultraviolet-Bright, High-Redshift ULIRGS

James W. Colbert[1], Harry Teplitz[1], Paul Francis[2], Povilas Palunas[3], Gerard M. Williger[4,5], Bruce Woodgate[6]

ABSTRACT

We present *Spitzer* Space Telescope observations of the z=2.38 Lyα-emitter over-density associated with galaxy cluster J2143-4423, the largest known structure (110 Mpc) above $z = 2$. We imaged 22 of the 37 known Lyα-emitters within the filament-like structure, using the MIPS 24μm band. We detected 6 of the Lyα-emitters, including 3 of the 4 clouds of extended ($>$50kpc) Lyα emission, also known as Lyα Blobs. Conversion from rest-wavelength 7μm to total far-infrared luminosity using locally derived correlations suggests all the detected sources are in the class of ULIRGs, with some reaching Hyper-LIRG energies. Lyα blobs frequently show evidence for interaction, either in *HST* imaging, or the proximity of multiple MIPS sources within the Lyα cloud. This connection suggests that interaction or even mergers may be related to the production of Lyα blobs. A connection to mergers does not in itself help explain the origin of the Lyα blobs, as most of the suggested mechanisms for creating Lyα blobs (starbursts, AGN, cooling flows) could also be associated with galaxy interactions.

Subject headings: galaxies: evolution, galaxies: high-redshift, infrared: galaxies

1. Introduction

The 110 Mpc filament mapped out by 37 Lyα-emitting objects around the $z = 2.38$ galaxy cluster J2143-4423 is the largest known structure above $z = 2$ (Palunas et al. 2004),

[1]Spitzer Science Center, California Institute of Technology, Pasadena, CA 91125

[2]Research School of Astronomy and Astrophysics, The Australian National University, Canberra, ACT 0200, Australia

[3]McDonald Observatory, University of Texas, Austin, TX 78712

[4]Dept. of Physics & Astronomy, University of Louisville, Louisville, KY 40292

[5]Dept. of Physics & Astronomy, John Hopkins University, Baltimore, MD 21218

[6]NASA Goddard Space Flight Center, Greenbelt, MD 20771

comparable in size to some of the largest structures seen in the local Universe (i.e. the Great Wall, Geller & Huchra 1989). Initially identified from narrow-band imaging tuned to Lyα at z=2.38, it has since been spectroscopically confirmed (Francis et al. 2004; Francis & Williger 2004). In addition to its compact Lyα-emitters, this high-redshift "Filament" is also home to four extended Lyα-emitting clouds, known more commonly as Lyman α blobs.

The Lyα blob is a relatively new class of objects found among high-redshift galaxy over-densities (Steidel et al. 2000; Keel et al. 1999; Palunas et al. 2004). While similar in extent ($\sim$100 kpc) and Lyα flux ($\sim 10^{44}$ ergs s^{-1}) to high-redshift radio galaxies, blobs are radio quiet and are therefore unlikely to arise from interaction with jets. Current surveys have reported the discovery of roughly 10 of these giant Lyα blobs, but they are not isolated high redshift oddities. Matsuda et al. (2004) have demonstrated that the blobs are part of a continuous size distribution of resolved ($>$16 arcsec^2) Lyα emitters, with more than 40 presently known.

One of the standing mysteries of the blobs is the source of their energy, as the measured ultraviolet flux from nearby galaxies is insufficient to produce the observed Lyα fluxes. One possibility is that the Lyα blobs are powered by supernova-driven superwinds (Ohyama & Taniguchi 2004), driving great plumes of gas into the surrounding ambient medium and producing shocks. An obscured AGN is another model, with the exciting ultraviolet illumination escaping along different lines of sight (i.e., Basu-Zych & Scharf 2004). Cooling flows have also been suggested (Fardal et al. 2001; Francis et al. 2001) as a possible power source.

There is growing evidence that Lyα blobs mark regions of extreme infrared luminosity. Submillimeter flux has been detected in two of the giant Lyα blobs, SMM J221726+0013 (Chapman et al. 2001) and SMM J17142+5016 (Smail et al. 2003). The submm source SMM J02399-0136 is also likely surrounded by a Lyα blob halo, as its Lyα emission covered most of a 15$''$ slit (Ivison et al. 1998). Most recently, Geach et al. (2005) has detected submm flux from four of the smaller (< 55 square arcsec) and less luminous ($< 2\times10^{43}$ L$_\odot$) Lyα blobs from Matsuda et al. (2004): LAB5, LAB10, LAB14 & LAB18. Also, Dey et al. (2005) has discovered a single Lyα blob (SST24 J1434110+331733) in the NOAO Deep Wide-Field Survey with strong 24μm flux (0.86 mJy).

In this paper we discuss the *Spitzer* 24μm observations of these z=2.38 Lyα-emitters, both compact sources and blobs. We estimate the total far-infrared luminosity for all detections and discuss the possibility of a connection between mergers and Lyα blobs. We assume an Ω_M=0.3, Ω_Λ=0.7 universe with H$_o$=70 km s^{-1} Mpc^{-1}.

2.   Observations

Our data were obtained using Multiband Imaging Photometer for Spitzer (MIPS; Rieke et al. 2004) in 24μm photometry mode. The field was observed on October 13 and 14 and November 4 and 5, 2004. The primary observation was a 3×5 raster map, covering approximately 15×25 arcminutes of the filament structure, centered at $21^h42^m38.0^s$, -44°26′30″. The total integration time per pixel is 1818 seconds. In addition we observed one small side field (5×5 arcmin) with a single known Lyα-emitter (at $21^h42^m56.3^s$, -44°37′57″) for 666 seconds. The data were initially reduced by the standard *Spitzer* pipeline [1]. We then produced sky frames for each data frame from the median of the 100 nearest (in time) data frames.

We assembled the final mosaic of the MIPS 24μm image using the MOPEX package available from the *Spitzer* Science Center. The final drizzled pixel scale is 1.23″ per pixel. For source extraction, we applied the APEX source extraction package available within MOPEX. APEX requires an input Point Response Function (PRF), which we created from the 40 brightest objects extracted from the final image. Our final APEX source extraction detected 3010 objects down to roughly 50 μJy. The full dataset will be discussed in a future paper.

The 5-σ detection limit, as measured within a 7.5″ aperture, is 58 μJy over most of the image, but can be as high as 180 μJy at the edges. None of the Lyα-emitters for which APEX failed to find MIPS sources had aperture fluxes greater than these 3-σ upper limits. A list of all extracted MIPS sources associated with Lyα-emitters is presented in Table 1. A brief note on the naming conventions: The first three Lyα-emitters were found by Francis et al. (1996) and named B1, B2, & B3. Further study by Francis et al. (1997) demonstrated that the B3 source was not real, but they also found another source, which they labeled B4. Palunas et al. (2004) found 34 additional Lyα-emitters in the field and so, rather than label each one, only gave B# designations to the three new Lyα blobs: B5, B6, & B7. We continue the B# naming convention, adding sources B8 and B9.

3.   MIPS Detections of Lyα Sources

Six out of 22 (∼30%) of the Lyα-emitters within the filament are associated with MIPS 24μm sources (Figure 1), including three of the four resolved (>50 kpc) Lyα blobs. This blob association rate is much higher than that for unresolved Lyα-emitters (Only 3 of 18). We determined a MIPS source to be associated if it lies within one MIPS FWHM (5.9″) of

---

the position of the Lyα-emitter. In four cases the coordinates for the MIPS and Lyα sources agree to less than an arcsecond, while the remaining two are separated by 2.7 (Blob B7) and 4.1$''$ (source B9). We checked the MIPS field astrometry against that of the optical data by comparing object centroids for all detected MIPS sources against those found in I-band. After correction for a 0.3$''$ offset, we found that the positions of the objects agree with a standard deviation of 1.5$''$.

The density of MIPS sources in the central portion of the field is $\sim$4.5 arcmin^{-2}, making the odds of a chance superposition of a random MIPS source $<$0.4% for those within an arcsecond, $< 2.9\%$ for within 2.7$''$, and $< 6.6\%$ for within 4.1$''$. However, all the detected Lyα-emitter counterparts have fluxes greater than 120 μJy, well above the detection limits and with a consequently lower surface density. Accounting for source brightness decreases the probability of chance superposition below 0.3% for all sources except for source B9, which has a 3.3% chance that its associated MIPS source (4.1$''$ away) is mere coincidence. For comparison, the Dey et al. (2005) MIPS source lies 2.5$''$ from the center of its associated Lyα blob.

We do not detect 16 of the 22 Lyα-emitters in the MIPS image. Six of these sources lie in regions of higher noise, where the 5σ detection limits range from 100-180 μJy. The remaining ten Lyα-emitters are in the central regions of the image, with detection limits of $<$60 μJy. The lack of faint MIPS counterparts is unlikely to be a result of error in object positions, as we examine a radius nearly 4 times the typical 1σ offset found from matching the MIPS and optical data. The absence of detections between 60 and 120 μJy indicates there is not a rapid climb in numbers with decreasing 24μm flux for Lyα-emitters over this range, although the number of objects considered is small.

Two of the Lyα blobs, B6 and B7, appear to have additional MIPS sources associated with them. The B6 Lyα blob extends over 25$''$, or over 200 kpc at z=2.38, and contains more than one knot or concentration. The brightest Lyα knot is the central one and it is associated with a bright MIPS source, but the southern knot (not to be confused with the large diffuse area to the southeast) also has a MIPS source of almost identical brightness. There is also an area of more diffuse Lyα emission to the north which also appears to be associated with a bright MIPS source. Each source is separted by approximately 9.5$''$ from the central source, creating a potential triple system. The northern source should probably be treated with some caution, as it not only lacks any clear Lyα concentration, but there is also a relatively bright galaxy visible at that location in the B-band image (B=22.5), which is unlikely to be at high redshift.

The center of the B7 Lyα blob actually lies between two sources. We have associated it with the brighter, closer MIPS source 2.7$''$ ($\sim$20 kpc) to its southeast, but a second source

lies $5.9''$ ($\sim$45 kpc) to the northwest. While there is a $\sim$10% chance the second object could be chance association, the location of the Lyα blob immediately between the two MIPS sources suggests a possible physical connection.

4. Ultraviolet-Bright ULIRGs

The detected 24μm flux densities range from 0.1 to 0.6 mJy, which at z=2.38 corresponds to roughly 2×10^{11} to 10^{12} L$_{\odot}$ in rest frame 7μm $\nu F\nu$. To convert from the mid-infrared to total bolometric luminosity (L$_{bol}$), we use the relationship from Chary & Elbaz (2001), hereafter CE01, calibrated by examining galaxies measured with both ISO and IRAS:

$$L_{IR} = 4.37^{+2.35}_{-2.13} \times 10^{-6} \times L_{6.7\mu m}^{1.62} \qquad (1)$$

In an effort to avoid over-estimation of L$_{IR}$, the mid-infrared conversion used throughout this paper assumes the low end of the 1σ envelope, producing total luminosities roughly a factor of 2 lower than a direct application of the formula. Even this conservative mid-IR conversion puts all the sources in the class of ultra luminous infrared galaxies (ULIRGs; $> 10^{12}L_{\odot}$), with many achieving Hyper-LIRG ($> 10^{13}L_{\odot}$) status (see Figure 2). It should be noted, however, that the CE01 relation is based on nearby starburst-dominated galaxies and it is possible it may not hold at high redshift or for the most extreme starbursts, if their spectral energy distributions are significantly different.

The L$_{bol}$ of most ULIRGs in the nearby universe comes from a combination of strong star formation and AGN activity (see Sanders & Mirabel 1996, for review). The majority are dominated by the stellar component, seen both in the far-infrared to radio relation (Yun, Reddy, & Condon 2001) and their strong PAH to continuum ratios (Lutz et al. 1998). However, this changes as the luminosity approaches that of the Hyper-LIRG (LIR$>10^{13}$ L$_{\odot}$); AGNs typically dominate above $\sim$10$^{12.5}$ L$_{\odot}$ (Tran et al. 2001). It is presently unknown how this trend will continue out to higher redshifts, where high-mass mergers, like those predicted to build giant ellipticals, could be producing energies on the scale of a Hyper-LIRG through star formation (Dopita et al. 2005). PAHs are already being found in high-redshift infrared sources (Houck et al. 2005; Yan et al. 2005). If these MIPS sources are AGN-dominated, one would expect $F_{\nu} \propto \nu^{-1}$, which would still place all the detected sources in the class of ULIRGs.

If we combine the 24μm detections from this study and from Dey et al. (2005) with the submm detections of Lyα blobs (Chapman et al. 2001; Smail et al. 2003; Geach et al. 2005), there are now at least 10 known high redshift ULIRGs surrounded by Lyα halos. We plot

Lyα luminosity versus L$_{bol}$ for all the identified Lyα blobs with infrared or submm detections in Figure 3. SMM J02399-0136 (Ivison et al. 1998) is excluded as its total Lyα flux is not precisely known. We use the published L$_{bol}$ values for all submm sources, but derive the total L$_{bol}$ for the Dey et al. (2005) 24μm source using the CE01 relation to better compare with our results.

Applying a similar analysis, Geach et al. (2005) found a weak Lyα/IR relation for submm-detected Lyα blobs with a typical L$_{Ly\alpha}$/L$_{bol}$ ratio just under 0.1%. Including our 24μm-detected Lyα blobs, which are brighter in Lyα than most of the Geach et al. (2005) objects, we continue to see the same weak trend, with a L$_{Ly\alpha}$/L$_{bol}$ efficiency of 0.05-0.2%. Neither the detection of X-rays (SMM J17142+5016 & LAB18) nor CIV emission (B1, SMM J17142+5016, & SST24 J1434110+331733), both strong indicators of AGN activity, has any clear effect on this trend. There is one significant outlier, the B5 blob, which falls at least a factor of 30 away from this proposed relation. While this relation is still tentative, it suggests a direct causal connection between the ULIRG infrared luminosity and the Lyα blobs.

5. Lyα Blob Merger Connection?

The high rate of MIPS detection for the Lyα blobs (3 out of 4) demonstrates that these ultraviolet sources are locations of tremendous infrared energy. Two of the Lyα blobs (B6 & B7) are associated with multiple MIPS sources, suggesting possible interaction or even merger. These separations between possible ULIRG component galaxies are large (60-70 kpc) compared to the typical low-redshift ULIRG, which have a median separation $\sim$2 kpc (Murphy et al. 1996). However, interacting ULIRGs with wide separations on the scale of 50 kpc do exist (Kim et al. 2002), and seem to occur when at least one the interacting galaxies is highly gas-rich (Dinh-V-Trung et al. 2001).

Previous high resolution *HST* imaging also indicates a possible Lyα blob connection to merging galaxies. For instance, NICMOS imaging of blob B1 shows a pair of compact, red galaxies with a projected separation of less than 7 kpc (Francis et al. 2001). Only three other Lyα blobs have been imaged with *HST*: the blobs in the field of 53W002, one of which shows a second nearby galaxy (Keel et al. 1999), and blob SSA22a-C11 (Steidel et al. 2000) which STIS imaging shows to be composed of several likely interacting components (Chapman et al. 2004). Dey et al. (2005) also find multiple components within their blob, visible in their ground-based, optical imaging.

In the local universe, the most energetic mergers are associated with the ULIRGs, with roughly 90% of ULIRGs clearly interacting (Bushouse et al. 2002; Farrah et al. 2001). The

majority of local ULIRG mergers are between two low mass (0.3-0.5 L*) galaxies (Colina et al. 2001), but major mergers of high-mass galaxies, like those predicted to build giant ellipticals, must be occurring at higher redshift (i.e., Conselice 2005). If merger-induced star formation is the source of the majority of the infrared flux in these objects, it implies star formation rates of 1000s of M$_\odot$ yr^{-1}, like those suggested for some sub-mm sources (Chapman et al. 2003; Geach et al. 2005). Such massive SFRs would be capable of generating the supernova kinetic energy needed to drive a superwind and power the Lyα blobs. If supernovas deposit roughly 10^{49} ergs per solar mass of stars into the surrounding medium (i.e., Bower et al. 2001), a star formation rate of 1000 M$_\odot$ yr^{-1} will easily match the $\sim 10^{51}$ ergs yr^1 emitted by the blobs, even at a low efficency.

Mergers could also help drive gas inwards into a supermassive black hole, making AGN another viable infrared energy source, with escaping ultraviolet radiation driving the Lyα blobs. Dey et al. (2005) found that their 24μm-detected blob is better fit by an AGN spectral energy distribution than that of a star forming galaxy, but longer rest-wavelengths or a mid-IR spectrum are required for a definitive determination. There is one clearly starbursting galaxy at the northern end of their Lyα nebula.

Cooling flows also remain a possibility, as it might be common to find multiple galaxies merging at the center of such a large inward flow of gas. It does become a less favored model, however, as the energy from the cooling gas in no longer required to power the Lyα blobs. The ULIRGs would appear to have more than enough energy in their budget to do so on their own.

REFERENCES

Basu-Zych, A. & Scharf, C. 2004, ApJL, 615, L85

Bower, R. G., Benson, A. J., Lacey, C. G., Baugh, C. M., Cole, S., & Frenk, C. S. 2001, MNRAS, 325, 497

Bushouse, H. A., et al. 2002, ApJS, 138, 1

Chapman, S. C., et al. 2004, ApJ, 606, 85

Chapman, S. C., Windhorst, R., Odewahn, S., Yan, H., & Conselice, C. 2003, ApJ, 599, 92

Chapman, S. C., Lewis, G., Scott, D., Richards, E., Borys, C., Steidel, C., Adelberger, K., & Shapley, A. 2001, ApJ, 548, L17

Chary, R., & Elbaz, D. 2001, ApJ, 556, 562

Colina, L., et al. 2001, ApJ, 563, 546

Conselice, C. J. 2005, ApJ, accepted, astro-ph/0405001

Dey, A., et al. 2005, ApJ, accepted, astro-ph/0503632

Dinh-V-Trung et al. 2001, ApJ, 556, 141

Dopita, M. A., et al. 2005, ApJ, 619, 755

Fardal, M. A., Katz, N., Gardner, J. P., Hernquist, L., Weinberg, D. H., & Davé, R. 2001, ApJ, 562, 605

Farrah, D., et al. 2001, MNRAS, 326, 1333

Francis, P. J., Palunas, P., Teplitz, H. I., Williger, G. M., & Woodgate, B. E. 2004, ApJ, 614, 75

Francis, P. J., & Williger, G. M. 2004, ApJL, 602, L77

Francis, P. J., et al. 2001, ApJ, 554, 1001

Francis, P. J., Woodgate, B., & Danks, A. 1997, ApJL, 482, L25

Francis, P. J., et al. 1996, ApJ, 457, 490

Geach, J. E., et al. 2005, submitted to MNRAS, astro-ph/0508357

Geller, M. J., & Huchra, J. P. 1989, Science, 246, 897

Houck, J. R., et al. 2005, ApJL, 622, L105

Ivison, R. J., Smail, I., Le Borgne, J.-F., Blain, A., Kneib, J.-P., Bezecourt, J., Kerr, T., & Davies, J. 1998, MNRAS, 298, 583

Keel, W. C., et al. 1999, AJ, 118, 2547

Kim, D. -C., Veilleux, S., & Sanders, D. B. 2002, ApJS, 143, 277

Lutz, D., et al. 1998, ApJL, 505, L103

Matsuda, Y., et al. 2004, AJ, 128, 569

Murphy, T., et al. 1996, AJ, 111, 1025

Ohyama, Y. & Taniguchi, Y. 2004, AJ, 127, 1313

Palunas, P., et al. 2004, ApJ, 602, 545

Rieke, G. H., et al. 2004, ApJS, 154, 25

Sanders, D. & Mirabel, I. 1996, ARAA, 34, 749

Smail, I., Ivison, R. J., Gilbank, D. G., Dunlop, J. S., Keel, W. C., Motohara, K., & Stevens, J.A. 2003, ApJ, 583, 551

Steidel, C. C., et al. 2000, ApJ, 532, 170

Tran, Q. D., et al. 2001, ApJ, 552, 527

Yan, L., et al. 2005, ApJ, 628, 604

Yun, M. S., Reddy, N. A., & Condon, J. J. 2001, ApJ, 554, 803

Table 1. Lyα Sources

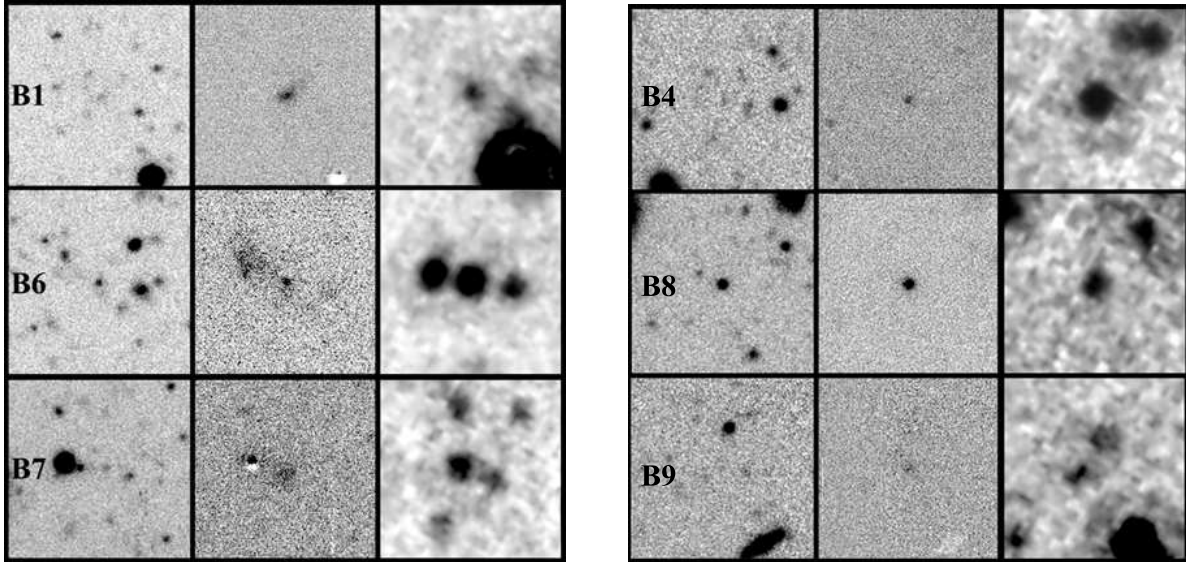| RA	Dec	log L$_{Ly\alpha}$ ergs s^{-1}	24μm F$_\nu$ μJy	νL_ν 10^{10} L$_\odot$	Total FIR 10^{10} L$_\odot$	Comment
21:42:27.59	-44:20:29.7	43.9	236	33.4	1000	Blob B1
21:42:32.16	-44:20:18.5	43.0	562	79.5	4300	B4
21:42:42.66	-44:30:09.4	43.8	634	89.5	5200	Blob B6
21:42:34.95	-44:27:08.8	43.5	292	41.3	1500	Blob B7; 2.7″ offset
21:43:05.84	-44:27:20.9	43.7	142	20.1	460	B8
21:43:37.33	-44:23:56.2	43.1	123	17.4	360	B9; 4.1″ offset
21:43:03.57	-44:23:44.2	43.8	< 58	< 8	< 80	Blob B5
Possible Lyα Blob Companions						
21:42:42.79	-44:30:18.2	n/a	535	76	3900	9.5″ from B6
21:42:42.49	-44:29:59.8	n/a	340	48	1900	9.5″ from B6
21:42:34.68	-44:27:01.2	n/a	172	24	620	5.9″ from B7

Fig. 1.— Left) Images of the 40″×40″ field around the three MIPS-detected Lyα blobs: B1, B6, & B7. From left to right the images are CTIO B-band, CTIO continuum-subtracted Lyα, and MIPS 24μm. East is upwards, north to the right. One arcsecond corresponds to 8kpc at z=2.38. Right) Images of the 40″×40″ field around the three MIPS-detected non-extended Lyα-emitters. Format is same as left.
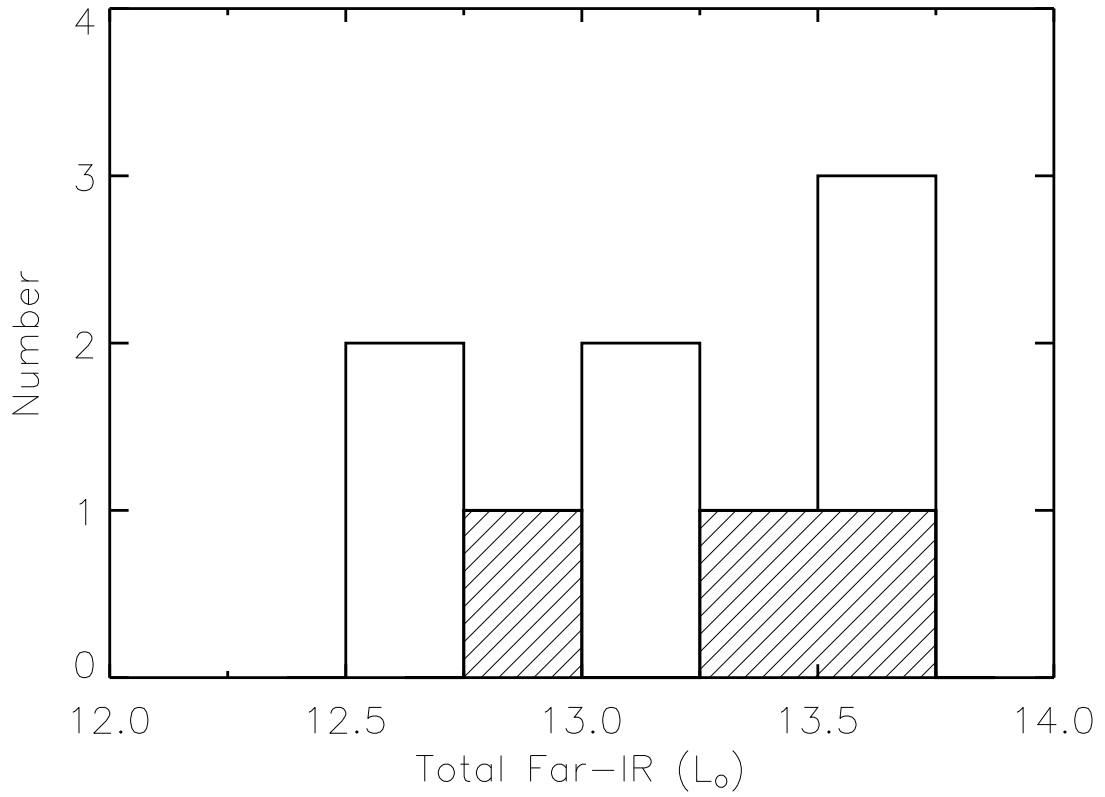
Fig. 2.— Histogram of inferred total far-infrared luminosity for MIPS sources associated with z=2.38 Lyα sources. The three sources potentially associated with the Lyα blobs B6 and B7 are marked with cross-hatching.
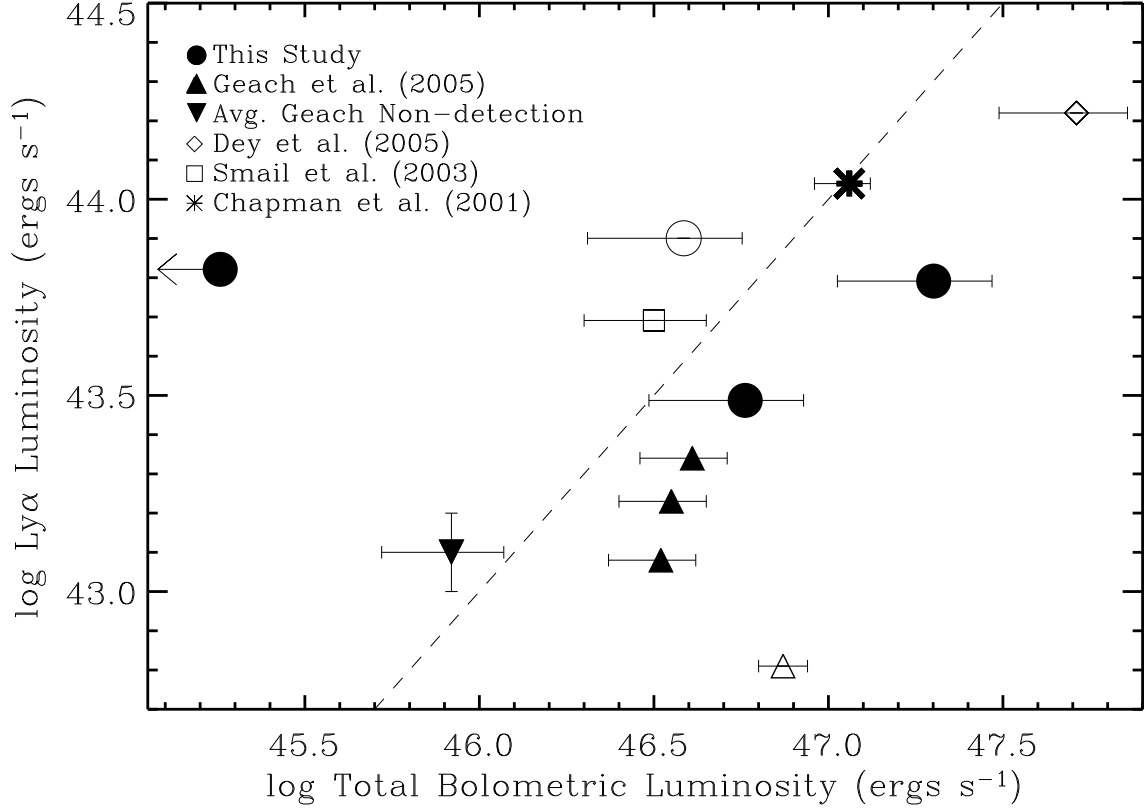
Fig. 3.— Log $L_{Ly\alpha}$ vs. log L_{bol} for high-z Lyα blob ULIRGs. The 24μm-detected blobs are the circles (This study) and the diamond (Dey et al. 2005), with error bars based on the estimated reliability of the Chary & Elbaz (2001) relation. The submm detections are the triangles (Geach et al. 2005), squares (Smail et al. 2003), and asterisks (Chapman et al. 2001). The upside-down triangle is the average of all non-detected Geach et al. blobs. Lyα blobs with evidence for AGN activity (X-rays or CIV emission) are plotted as hollow symbols. The dashed line marks where $L_{Ly\alpha}/L_{bol} = 0.001$.